J. Fluid Mech. (2001), *vol.* 435, *pp.* 93–102. Printed in the United Kingdom

© 2001 Cambridge University Press

Exact coherent structures in channel flow

By FABIAN WALEFFE

Departments of Mathematics and Engineering Physics, 819 Van Vleck Hall,
University of Wisconsin, Madison WI 53706, USA

(Received 16 December 2000 and in revised form 1 February 2001)

Exact coherent states in no-slip plane Poiseuille flow are calculated by homotopy from free-slip to no-slip boundary conditions. These coherent states are unstable travelling waves. They consist of wavy low-speed streaks flanked by staggered streamwise vortices closely resembling the asymmetric coherent structures observed in the near-wall region of turbulent flows. The travelling waves arise from a saddle-node bifurcation at a sub-turbulent Reynolds number with wall-normal, spanwise and streamwise dimensions smaller than but comparable to 50^+, 100^+ and 250^+, respectively. These coherent solutions come in pairs with distinct structure and instabilities. There is a three-dimensional continuum of such exact coherent states.

1. Introduction

Landau (1944) wrote 'Although turbulent motion has been extensively discussed in the literature, the very essence of the phenomenon is still lacking sufficient clearness. In the author's opinion, the problem may appear in a new light if the process of initiation of turbulence is examined thoroughly'.

Well-known routes to chaos have since been discovered but the onset of turbulence in the most basic type of turbulent flow, such as flow in pipes or channels, is still not understood today. In fact, contrary to Landau's opinion, studies of turbulence and turbulence onset in wall-bounded shear flows have typically proceeded independently in the fluid dynamics literature, with authors focusing either on the statistical flow properties at high Reynolds number or on transition from laminar flow at 'low' Reynolds number. Over the last four decades, a lot of research has taken place in a third area devoted to the study of coherent structures observed in the near-wall region of wall-bounded turbulent flows at low to moderate Reynolds numbers. Recent overviews of that research area can be found in the monographs by Holmes, Lumley & Berkooz (1996) and Panton (1997).

An objective of this and earlier work is to establish a link between the onset of shear turbulence and the coherent structures. The physics underlying the coherent structures was isolated and identified as a fundamental self-sustaining process for shear flows in Hamilton, Kim & Waleffe (1995) and Waleffe (1995, 1997). A definite demonstration of the validity of that self-sustaining process was the calculation of three-dimensional unstable steady states in plane Couette flow by a method directly tied to the process (Waleffe 1998). That method consisted of the smooth continuation of steady states from a two-dimensional 'streaky' flow, with streamwise rolls externally maintained by a weak $O(Re^{-2})$ forcing, to a fully three-dimensional flow with self-sustained staggered nearly streamwise vortices. The plane Couette solutions were then smoothly deformed into travelling wave solutions in plane Poiseuille flow. Those calculations were made for Neumann boundary conditions (free-slip perturbations).

https://doi.org/10.1017/S0022112001004189 Published online by Cambridge University Press

In this paper, we extend those solutions to no-slip plane Poiseuille flow by homotopy from free-slip to no-slip boundary conditions. These three-dimensional travelling waves are non-trivial solutions of the Navier–Stokes equations that are very similar to the coherent structures observed in experiments and numerical simulations. They exist without any of the complex spatio-temporal intermittency characteristic of coherent structures observed in turbulent flows, hence they can be considered as 'pure' or 'exact' coherent structures. We choose the term *exact coherent structures* to emphasize that these are fundamental solutions of the Navier–Stokes equations that provide a rigorous basis for the notions of 'active' and 'inactive motions' often used in the coherent structure literature. The further study of these solutions and their spatio-temporal instabilities is thought to be a promising route for improving our understanding of shear turbulence.

2. Mathematical and numerical formulation

The mathematical problem consists of the Navier–Stokes equations for the solenoidal velocity field $\boldsymbol{v}(\boldsymbol{x},t)$ in the slab $-1 \leqslant y \leqslant 1$ with periodicity in the streamwise x and spanwise z directions. The periodic lengths are $L_x = 2\pi/\alpha$ and $L_z = 2\pi/\gamma$ respectively. Results shown here are for $\alpha = 0.5$ and $\gamma = 1.5$. Pressure is eliminated by the poloidal–toroidal projection of the Navier–Stokes equations. The dynamical variables are the wall-normal velocity $v(\boldsymbol{x},t)$ and vorticity $\eta(\boldsymbol{x},t)$ together with the mean flow $\bar{u}(y,t)$. The complete velocity field is decomposed into its laminar part $U_L(y) = y - y^2/2 + 1/6$ and a perturbation $\boldsymbol{u}(\boldsymbol{x},t)$. This corresponds to a half-plane Poiseuille flow with the bottom wall at $y = -1$ and the channel centreline at $y = 1$ in a frame moving with the average laminar velocity (see figure 2*a*). The Reynolds number Re is therefore based on one quarter of the full channel height H ($h = H/4$) and the imposed pressure gradient $\mathrm{d}P/\mathrm{d}x$ such that $Re = |\mathrm{d}P/\mathrm{d}x|h^3/\nu^2$. In these units, the friction velocity $u_\tau = (2/Re)^{1/2}$, kinematic viscosity $\nu = 1/Re$ and the friction Reynolds number based on the half-channel height is $R_\tau = (8Re)^{1/2}$.

The half-Poiseuille flow with the unusual normalization $U_L(y) = y - y^2/2 + 1/6$ is chosen because it is closest to the plane Couette flow $U(y) = y$ (the antisymmetric parts are identical and the symmetric parts have zero average). These choices are motivated by the underlying self-sustaining process and the solution procedure. The latter consists of tracking travelling wave solutions for the flow $U_L(y) = y + \mu(1/6 - y^2/2)$, as a function of μ, from the three-dimensional steady states in plane Couette flow at $\mu = 0$ to plane Poiseuille flow at $\mu = 1$ (homotopy). For continuation from free-slip perturbations to no-slip we consider the general slip boundary conditions

$$\lambda u + (\lambda - 1)\frac{\partial u}{\partial y} = v = \lambda w + (\lambda - 1)\frac{\partial w}{\partial y} = 0 \tag{2.1}$$

at $y = -1$ (bottom wall) and $\partial u/\partial y = v = \partial w/\partial y = 0$ at $y = 1$ (centreline).

We look for travelling wave solutions of the form $\boldsymbol{u}(\boldsymbol{x},t) = \boldsymbol{u}(x - Ct, y, z)$. Substituting this expression in the Navier–Stokes equations $\partial\boldsymbol{u}/\partial t + \boldsymbol{F}(\boldsymbol{u}) = 0$ leads to the time-independent nonlinear problem $\boldsymbol{F}(\boldsymbol{u}) - C\partial\boldsymbol{u}/\partial x = 0$, where the convection velocity C is essentially a nonlinear eigenvalue. A unique solution is obtained by arbitrarily fixing the phase of the solution. In the present calculations we set $\mathrm{Im}\langle\eta \mathrm{e}^{-\mathrm{i}\alpha x}\rangle = 0$ where $\langle\cdot\rangle$ denotes a volume average. This differs by a $\pi/2$ phase shift from the normalization $\mathrm{Im}\langle w \mathrm{e}^{-\mathrm{i}\alpha x}\rangle = 0$ used in Waleffe (1998). The equations $\boldsymbol{F}(\boldsymbol{u}) - C\partial\boldsymbol{u}/\partial x = 0$ and $\mathrm{Im}\langle\eta \mathrm{e}^{-\mathrm{i}\alpha x}\rangle = 0$ determine a three-dimensional manifold of travelling wave solutions parametrized by α, γ, Re. The equations are discretized as discussed below and the

https://doi.org/10.1017/S0022112001004189 Published online by Cambridge University Press

resulting nonlinear algebraic problem is solved by Newton's method. A good guess for the Newton iterations is generated by homotopy from free-slip solutions at $\lambda = 0$ to no-slip at $\lambda = 1$. Ten or fewer equal λ-steps are sufficient. The solutions have been mapped as easily from free-slip Couette flow by setting $\lambda = \mu = 0 \rightarrow 1$. A similar continuation from free-slip to no-slip for the upper wall can be used to extend the solutions to no-slip plane Couette flow and one recovers the steady states discovered by Nagata (1990) and studied by Clever & Busse (1992, 1997). All these solutions in free-slip, slip, and no-slip plane Couette and Poiseuille flows are therefore directly connected.

The numerical discretization employs Fourier modes in the x- and z-directions. The y-expansion is based on Chebyshev integration. The highest derivatives are expanded in Chebyshev polynomials and then Galerkin expansion functions are constructed by integration using the boundary conditions. Care must be taken to define expansion functions that are smooth in λ and extend to free-slip where the second-order differential operator is singular. Besides providing excellent numerical conditioning (Greengard 1991), this approach automatically satisfies the boundary conditions. This formulation thus enforces all kinematic constraints (solenoidality and boundary conditions) *ab initio*. This reduces the size of the nonlinear problem that must be solved. The expansions are truncated using an ellipsoidal cut-off as in Waleffe (1998). If (l, m, n) are the Fourier–Chebyshev indices corresponding to the x, y, z expansions, respectively, then modes with $l^2/(L_T+1)^2 + m^2/(M_T+1)^2 + n^2/(N_T+1)^2 \geqslant 1$ are truncated, where (L_T, M_T, N_T) specifies the resolution. This resolution approximately corresponds to a full channel simulation with resolution $(2L_T+1) \times 2(M_T+5) \times 2(N_T+1)$ after de-aliasing in x and z. The governing equations are projected onto each Chebyshev and Fourier mode. There is no aliasing in x and z (fully spectral approach). De-aliasing in y made no difference on the scale of the plots shown here. The size of the problem is further reduced by imposing the symmetry

$$\begin{pmatrix} u \\ v \\ w \end{pmatrix}(x, y, z) = \begin{pmatrix} u \\ v \\ -w \end{pmatrix}\left(x + \frac{L_x}{2},\, y,\, -z\right) \tag{2.2}$$

which arises from the sinusoidal instability of streaks (Waleffe 1995, 1997).

All free-slip results obtained with a different triply Fourier code were reproduced with the present code. The linear instability of two-dimensional streaky flow was also reproduced as well as eigenmodes of the Orr–Sommerfeld and Squire operators. The highest resolution shown here, $(11, 23, 11)$, corresponds to 7391 modes. For the highest Reynolds number shown here, $Re = 423$, and $\alpha = 0.5$ ($L_x^+ \approx 365$), $\gamma = 1.5$ ($L_z^+ \approx 122$), that resolution corresponds to $\Delta x^+ \approx 16$, $\Delta z^+ \approx 5$ and the first two Gauss–Chebyshev points at $y^+ \approx 0.046$ and 0.4, respectively. The lowest resolution (one of the solid curves in figure 1) is $(9, 17, 9)$ which corresponds to 3889 modes.

3. Results

Homotopy from a free-slip solution to no-slip provides one point on the three-dimensional manifold of travelling wave solutions. Figure 1 shows part of a one-dimensional curve corresponding to $\alpha = 0.5$, $\gamma = 1.5$ on that manifold. The results are displayed in terms of the non-dimensional pressure gradient R_P ($= 8R_\tau^2 = 64Re$) and the non-dimensional total volume flow rate per unit spanwise width R_Q. The travelling wave solutions arise from a saddle-node bifurcation at $Re \approx 252$ ($R_\tau \approx 45$ or $R_Q \approx 887$) for $\alpha = 0.5$ and $\gamma = 1.5$. For higher Re there are two solutions,

https://doi.org/10.1017/S0022112001004189 Published online by Cambridge University Press

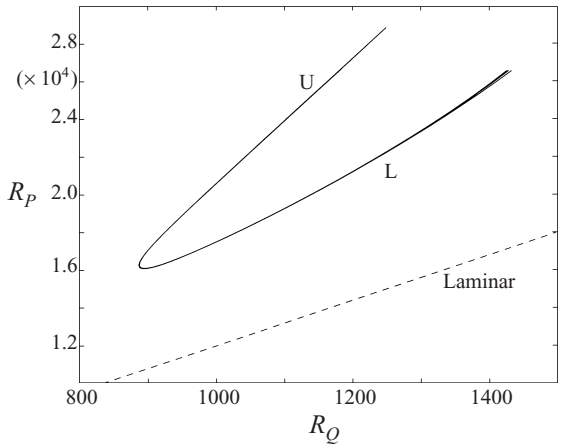


FIGURE 1. Bifurcation diagram: $R_Q = Q/\nu$, $R_P = |\mathrm{d}P/\mathrm{d}x|H^3/\nu^2$, $Q = \langle u - u_{wall}\rangle H$; dashed line is laminar state $R_P = 12R_Q$, solid lines are the pair of exact three-dimensional coherent states at $\alpha = 0.5$, $\gamma = 1.5$. Five resolutions are plotted but they closely overlap, demonstrating convergence.

an upper branch and a lower branch. The upper branch is defined as the solution which is furthest from laminar. Five different resolutions are plotted in figure 1: $(L_T, M_T, N_T) = (9, 17, 9)$, $(9, 21, 11)$, $(9, 23, 11)$, $(9, 23, 13)$ and $(11, 23, 11)$. The three-dimensional solutions extend to higher Reynolds numbers than shown in figure 1. The structure of the three-dimensional travelling waves depends continuously on the Reynolds number and horizontal wavenumbers α and γ. A surprising result is that the convergence on the lower branch is not as good as on the upper branch. This is counter-intuitive as the lower branch is closer to laminar hence 'less non-linear'. The reason is that the lower branch has smaller x-dependence but finer y, z structure.

The mean velocity profiles for the upper branch solution at $Re = 423$ and the lower branch at $Re = 415$, both corresponding to $R_\tau \approx 58$, are shown in figure 2(a). Note the two slight inflections in the profiles. The centreline velocities for the upper and lower branch solutions are -0.465 and -0.258, respectively. These profiles are displayed on a log–lin plot in wall units in figure 2(b). The exact coherent structure profiles have a kink that occurs in between the two inflection points of the profile. The kink is centred at the location not of the maximum (Sreenivasan & Sahay 1997) but of the inflection in the Reynolds stress profile corresponding to most negative slope. The maximum occurs at $y \approx -0.3$ ($y^+ \approx 20$) and the inflection point at $y \approx 0.4$ ($y^+ \approx 40$). Malkus & Smith (1989) obtained realistic profiles with a kink in their optimum 'efficiency function' results although their mean profile was constrained to have negative semi-definite curvature.

The dashed line in figure 2(b) is the Kim, Moin & Moser (1987) turbulent mean profile calculated at $R_\tau = 180$. Although the R_τ values are different, this comparison allows the speculation that turbulent flows are statistically 'in between' the upper branch and the lower branch solutions. The upper branch provides an upper bound on flow rate reduction (or drag increase) while the lower branch may provide a lower bound. Turbulence reduces drag when compared to the upper branch solution.

The convection velocity C (not shown) is a function of α, γ, Re. Near the bifurcation point ($Re \approx 252$ for $\alpha = 0.5$, $\gamma = 1.5$) $C \approx -0.30$ while $C \approx -0.31$ for the lower branch at $Re = 415$ and $C \approx -0.55$ for the upper branch at $Re = 423$. In wall

https://doi.org/10.1017/S0022112001004189 Published online by Cambridge University Press

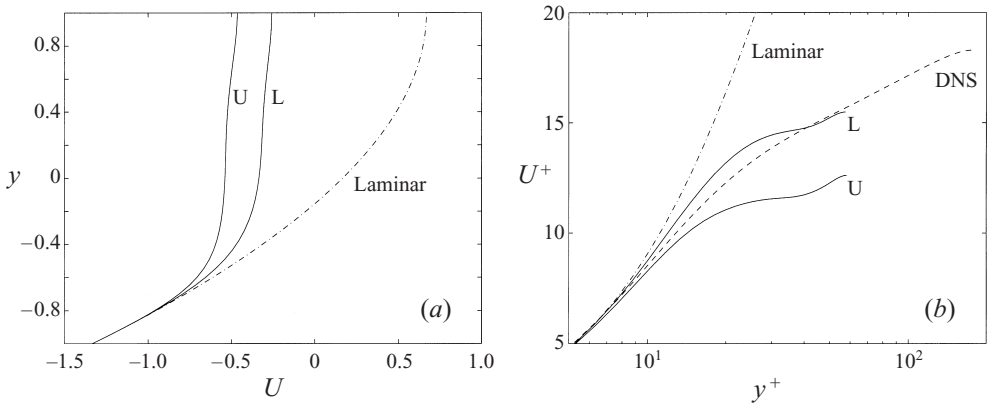


FIGURE 2. Mean flow $\bar{U}(y)$ for upper and lower three-dimensional states at $R_\tau \approx 58$, $\alpha = 0.5$, $\gamma = 1.5$. DNS in (*b*) is Kim *et al.*'s (1987) $R_\tau = 180$ data.

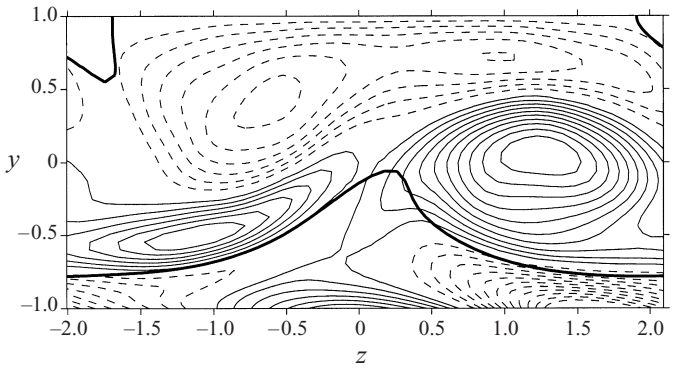


FIGURE 3. Upper branch at $Re = 376$ ($R_\tau \approx 55$, $L_z^+ \approx 115$). Level curves of streamwise vorticity ω_x at $\alpha x = 3\pi/2$ (solid: positive, dashed: negative. Twenty-two equispaced levels between $\pm\max[\omega_x(x,y,z)]$. Min $[\omega_x(x,y,z)]$ is at the no-slip wall at $y = -1$, $z \approx 1.5$.) Thick lines are level curves $u = \min[u(x, y = 0, z)]$ and $\max[u(x, y = 0, z)]$.

units, the latter two velocities are $(C - U_{wall})/u_\tau \approx 15$ and 11, respectively. These velocities correspond approximately to the mean velocity at the first inflection point (minimum slope) of the mean flow (near $y = 0$, or $y^+ \approx 30$). This is consistent with the self-sustaining process in which the central mechanism is the instability of the streaks. That instability is driven primarily by the spanwise inflections in the x-averaged streamwise velocity. The maximum spanwise shear occurs roughly at the distance from the wall where the mean profile achieves its minimum slope.

Figure 3 is a y, z cut of the upper branch solution at $Re = 376$ ($R_\tau \approx 55$, $L_z^+ \approx 115$) that should be compared with the corresponding free-slip plane Couette and Poiseuille solutions (figures 4 and 5 in Waleffe 1998). The no-slip boundary condition, in effect, reduces the height of the channel. This suggests that a 'better' solution, in the sense of surviving to lower Reynolds number, may be obtained by reducing L_z (and consequently L_x as the two are linked by an optimum ratio somewhere between 2 and 3 through the streak instability, see e.g. Waleffe 1995, 1997; Waleffe & Kim 1998).

Figures 4 and 5 illustrate the structure of both branches. The upper branch (figure 4) consists of wavy streaks with staggered nearly streamwise vortices. This is very similar to the coherent structure sketched by Stretch (1990) (figure 1 in Waleffe 1998). These

https://doi.org/10.1017/S0022112001004189 Published online by Cambridge University Press

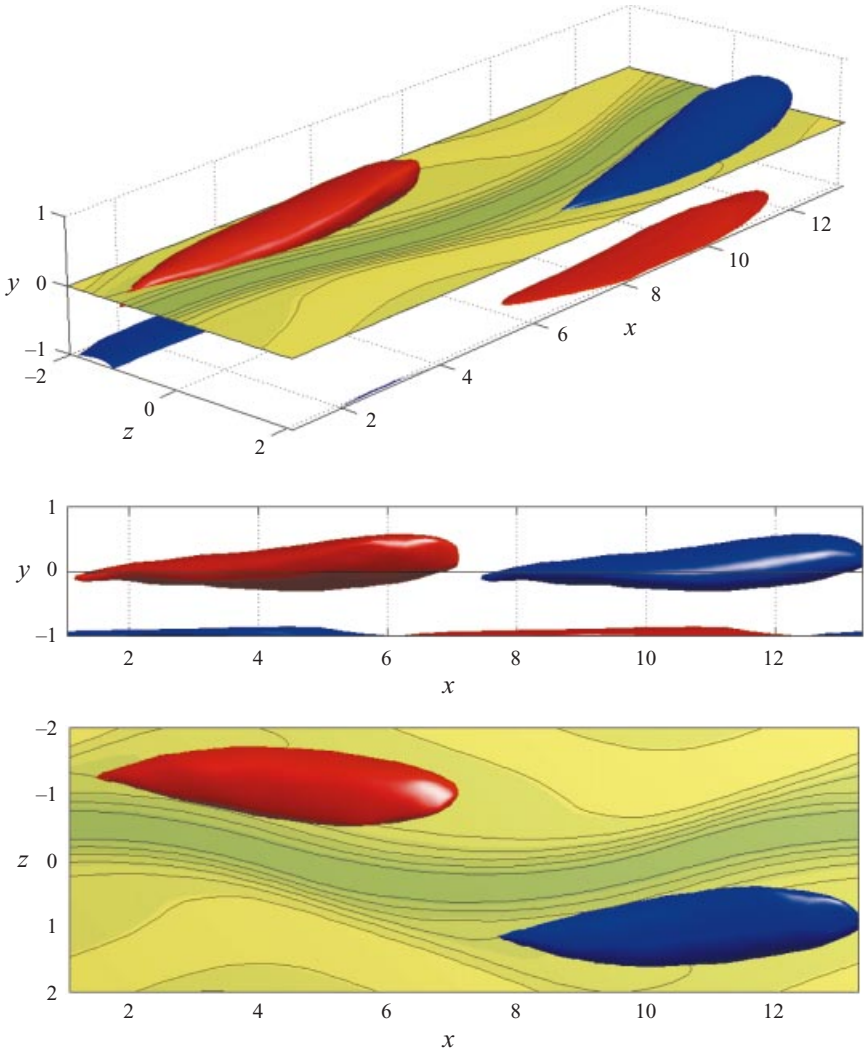


FIGURE 4. Perspective, side and top view of level curves of streamwise velocity u at $y = 0$ overlayed with isosurfaces of streamwise vorticity ($\pm 60\%$ max$[\omega_x(x, y, z)]$, the maximum occurs at the wall). Positive vorticity blue, negative red. Upper branch at $Re = 376$, $R_\tau \approx 55$. Flow is toward positive x.

solutions are virtually identical to the free-slip solutions except for extra high-vorticity regions at the wall, below the vortices, in the no-slip case and an additional symmetry in plane Couette flow. The lower branch solution (figure 5) develops a distinct and more complex structure. The lower branch streaks are stronger and less wavy than in the upper branch solution. They are flanked by staggered nearly streamwise vortices that split into two pieces, one of which straddles the streak. A second set of similar vortices, slightly weaker and shifted by about half a period, also exists.

Both of these branches of solutions are unstable to perturbations with the same wavelengths and symmetry. The unstable eigenvalues consists of a complex conjugate pair and one real eigenvalue on the lower branch and a complex conjugate pair on the upper branch. The real part of the complex pair on the upper branch is almost independent of Re, for the range of Re presented here ($252 \leqslant Re \leqslant 423$), with a

https://doi.org/10.1017/S0022112001004189 Published online by Cambridge University Press

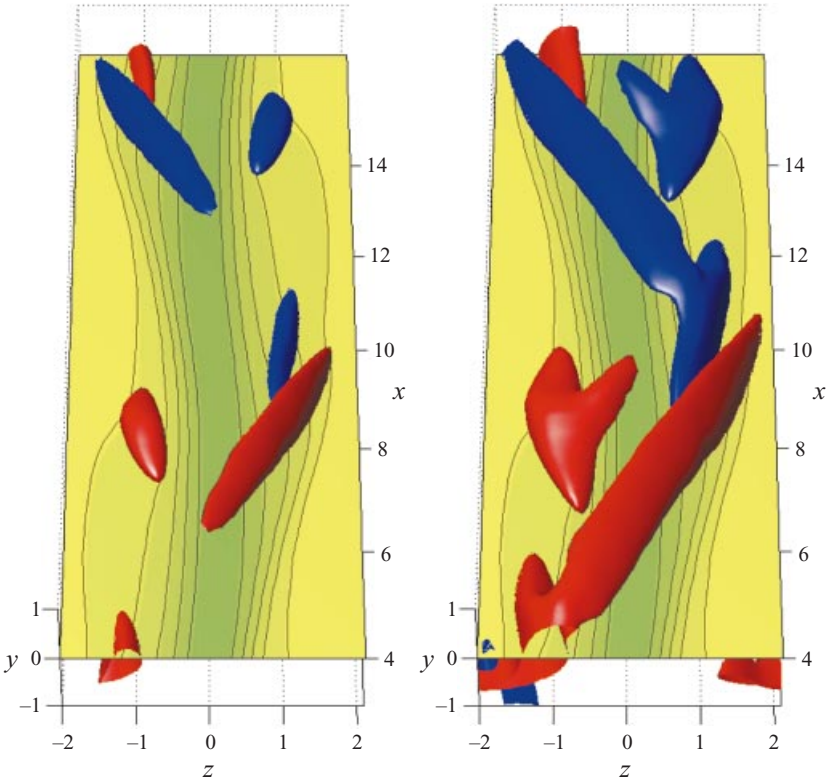


FIGURE 5. Lower branch at $Re = 415$ ($R_\tau \approx 58$). Level curves of streamwise velocity u at $y = 0$ overlayed with isosurfaces of streamwise vorticity (Left: $\pm 60\%\ \max[\omega_x(x, y, z)]$), right: $\pm 40\%\ \max[\omega_x(x, y, z)]$).

value ≈ 0.014. The lower branch is more unstable, with the real eigenvalue quickly dominating and reaching ≈ 0.04 at $Re = 415$. Both travelling wave solutions are thus saddle solutions. Presumably, there exist also subharmonic and symmetry-breaking instabilities.

4. Discussion

These instabilities do not imply that the exact coherent states are physically irrelevant, quite the contrary. In experiments, coherent structures are observed only intermittently, in space and time, embedded in a sea of 'turbulence' and transition is known to be a complex spatio-temporal process as well. The exact coherent states and their instabilities provide a potentially fruitful decomposition of the flow. Some of these instabilities, and associated bifurcations, will correspond to a different dynamical manifestation (e.g. time-periodic solutions) of the same underlying self-sustaining process while others will correspond to instabilities leading to 'cascades', not to self-sustained structures. The subharmonic instabilities are probably linked to spatio-temporal disorder and to spots in transitional flow. Recent simulations and experiments in plane Couette flow on turbulence onset and its connections with coherent structures have been performed by Schmiegel & Eckhardt (1997) and Bottin

https://doi.org/10.1017/S0022112001004189 Published online by Cambridge University Press

et al. (1998). Grossmann (2000) reviews a different approach based on the laminar flow and linear transient growth (see also Schmid 2000).†

Recent work on exact coherent states and their instabilities has been done by Toh & Itano (1999). These authors not only linked the fundamental instability of the travelling wave solutions to 'bursting', but also managed to approach the unstable travelling wave itself using direct numerical simulations (DNS) and a shooting method based on the two-dimensional–three-dimensional decomposition inherent in the conceptual formulation of the self-sustaining process (e.g. Hamilton *et al.* 1995; Waleffe 1997). The solution approached by Toh & Itano (1999) (see also Itano & Toh 2001) is presumably analogous to the lower branch of solutions illustrated here. Their travelling wave is localized near one wall, however, while ours are symmetric across the centreline. Hence their travelling wave is probably a distinct nonlinear object, although the underlying physics is undoubtedly the same self-sustaining process. The success of their shooting procedure also suggests that their travelling wave has only one real unstable eigenvalue as opposed to one real and one complex conjugate pair for the lower branch here. Toh & Itano impose constant mass flux, however, while we use constant pressure gradient. This affects the stability characteristics and may explain why the unstable eigenvalues would differ by a complex conjugate pair.

The manner in, and conceptual ease with which, the exact coherent structures shown here have been constructed, from a streamwise-independent streaky flow to free-slip plane Couette to free-slip Poiseuille to no-slip Poiseuille (and to no-slip Couette), demonstrates the close connections between the exact coherent structures in these various flows and the underlying self-sustaining process.‡ This close connection is confirmed by inspection of the structure of the solutions which corresponds in all cases to wavy streaks flanked by staggered nearly streamwise vortices. The exact coherent structures are literally a few steps away from each other (in the homotopy parameters λ and μ). These results demonstrate unequivocally that the underlying self-sustaining process is robust and independent of the generation of vorticity at the wall by viscosity, of interaction with an 'outer' flow and of how exactly the mean shear is maintained. Our series of results in this and earlier work contradicts the claims in Schoppa & Hussain (1997) that the self-sustaining processes and structures in Couette and Poiseuille flows are fundamentally different. Recent work by Jimenez & Pinelli (1999) confirms many of these points about the nature of the underlying self-sustaining process. Jimenez & Pinelli (1999) do so through DNS using, in particular, a filtering scheme that effectively wipes out all fluctuations beyond a certain distance from the wall but has no effect in the near-wall region. This suggests that the near-wall region is indeed 'autonomous', although there remains some interaction with an outer layer, whose dynamics is governed not by the Navier–Stokes equations but by suitably filtered equations, and that interaction probably affects the dynamics if not so much the structures themselves. In our work, there is an extra no-slip or free-slip wall that absolutely prevents interaction with any outer flow. The exact coherent structures that have been found can be continued to higher Reynolds number and

† The main transient algebraic growth is the 'linearized' representation of the formation of streaks by streamwise rolls, the simplest part of the self-sustaining process (Waleffe 1995, 1997). The 'optimum' streaky flows selected by that linearized approach do not have the proper structure and strength to serve as starting points for the calculation of the self-sustained states.

‡ The wall may not even be necessary and one expects self-similar versions of these exact coherent structures in free shear layers. Sreenivasan (1988) argued in a similar vein that the large-scale structure in wall-bounded and free shear flows have the same origin.

https://doi.org/10.1017/S0022112001004189 Published online by Cambridge University Press

this is equivalent, in wall units, to moving that 'extra' wall away from the bottom wall.

5. Conclusions

Exact coherent structures in plane Poiseuille flow with no-slip boundary conditions have been calculated from the Navier–Stokes equations. These solutions are unstable travelling waves that were obtained by homotopy from free-slip Couette or Poiseuille solutions. The upper branch of these exact coherent structures is remarkably similar to the asymmetric coherent structures first educed from turbulent channel flow and sketched by Stretch (1990), but the exact coherent structures are not embedded in a sea of turbulent disorder and survive down to Reynolds numbers where turbulence is not observed. The lower branch evolves into a related but more complex structure. The mean profiles of these travelling waves have an interesting structure with a kink and a hint, perhaps, of a 'log' layer even at this absurdly low $R_\tau \approx 50$. These profiles suggest that the upper branch solution provides a realizable upper bound on drag increase (or flow reduction) while the lower branch may provide a lower bound. This provides strong evidence for the notion, suggested long ago by upper bound theories (e.g. Malkus & Smith 1989), that momentum transport and turbulent disorder are two distinct issues. It may be that the upper branch travelling wave solutions are the most efficient momentum transporting motions allowed by the Navier–Stokes equations and that the instabilities feeding on these coherent solutions sustain the turbulent disorder but reduce momentum transport.

The author is grateful for support provided by NSF award DMS-9803685.

REFERENCES

Bottin, S., Daviaud, F., Manneville, P. & Dauchot, O. 1998 Discontinuous transition to spatio-temporal intermittency in plane Couette flow. *Europhys. Lett.* **43**, 171–176.

Clever, R. M. & Busse, F. H. 1992 Three-dimensional convection in a horizontal layer subjected to constant shear. *J. Fluid Mech.* **234**, 511–527.

Clever R. M. & Busse, F. H. 1997 Tertiary and quaternary solutions for plane Couette flow. *J. Fluid Mech.* **344**, 137–153.

Greengard, L. 1991 Spectral integration of two-point boundary value problem. *SIAM J. Numer. Anal.* **28**, 1071–1080.

Grossmann, S. 2000 The onset of shear turbulence. *Rev. Mod. Phys.* **72**, 603–618.

Hamilton, J. M., Kim, J. & Waleffe, F. 1995 Regeneration mechanisms of near-wall turbulence structures. *J. Fluid Mech.* **287**, 317–348.

Holmes, P., Lumley, J. L. & Berkooz, G. 1996 *Turbulence, Coherent Structures, Dynamical Systems and Symmetry*. Cambridge University Press.

Itano, T. & Toh, S. 2001 The dynamics of the bursting process in wall turbulence. *J. Phys. Soc. Japan* **70**, 701–714.

Jimenez, J. & Pinelli, A. 1999 The autonomous cycle of near-wall turbulence. *J. Fluid Mech.* **389**, 335–359.

Kim, J., Moin, P. & Moser, R. D. 1987 Turbulence statistics in fully developed channel flow at low Reynolds number. *J. Fluid Mech.* **177**, 133–166.

Landau, L. D. 1944 On the problem of turbulence. *Akad. Nauk. Dokl.* **44**, 339. Reprinted in *Chaos* (ed. B.-L. Hao), pp. 107–111. World Scientific (1984).

Malkus, W. V. R. & Smith, L. M. 1989 Upper bounds on functions of the dissipation rate in turbulent shear flow. *J. Fluid Mech.* **208**, 479–507.

Nagata, M. 1990 Three-dimensional finite-amplitude solutions in plane Couette flow: bifurcation from infinity. *J. Fluid Mech.* **217**, 519–527.

https://doi.org/10.1017/S0022112001004189 Published online by Cambridge University Press

Panton, R. L. (Ed.) 1997 *Self-Sustaining Mechanisms of Wall Turbulence*. Computational Mechanics Publications, Southampton.

Schmid, P. J. 2000 Linear stability theory and bypass transition in shear flows. *Phys. Plasmas* **7**, 1788–1794.

Schmiegel, A. & Eckhardt, B. 1997 Fractal stability border in plane Couette flow. *Phys. Rev. Lett.* **79**, 5250–5253.

Schoppa, W. & Hussain, F. 1997 Genesis and dynamics of coherent structures in near-wall turbulence: a new look. In *Self-Sustaining Mechanisms of Wall Turbulence* (ed. R. L. Panton), pp. 385–422. Computational Mechanics Publications, Southampton.

Sreenivasan, K. R. 1988 A unified view of the origin and morphology of the turbulent boundary layer structure. In *Turbulence Management and Relaminarisation* (ed. H. W. Liepmann & R. Narasimha), pp. 37–61. Springer.

Sreenivasan, K. R. & Sahay, A. 1997 The persistence of viscous effects in the overlap region and the mean velocity in turbulent pipe and channel flows. In *Self-Sustaining Mechanisms of Wall Turbulence* (ed. R. L. Panton), pp. 385–422. Computational Mechanics Publications, Southampton.

Stretch, D. D. 1990 Automated pattern eduction from turbulent flow diagnostics. *Annual Research Briefs-1990*, pp. 145–157. Center for Turbulence Research, Stanford University.

Toh, S. & Itano, T. 1999 Low-dimensional dynamics embedded in a plane Poiseuille flow turbulence: Traveling-wave solution is a saddle point? *Proc. IUTAM Symp. on Geometry and Statistics of Turbulence* (ed. T. Kambe). Kluwer (in press).

Waleffe, F. 1995 Hydrodynamic stability and turbulence: beyond transients to a self-sustaining process. *Stud. Appl. Maths* **95**, 319–343.

Waleffe, F. 1997 On a self-sustaining process in shear flows. *Phys. Fluids* **9**, 883–900.

Waleffe, F. 1998 Three-dimensional coherent states in plane shear flows. *Phys. Rev. Lett.* **81**, 4140–4143.

Waleffe, F. & Kim, J. 1998 How streamwise rolls and streaks self-sustain in a shear flow: Part 2. *AIAA Paper* 98-2997.

https://doi.org/10.1017/S0022112001004189 Published online by Cambridge University Press